Int. J. Heat Mass Transfer. Vol. 14, pp. 1787–1805. Pergamon Press 1971. Printed in Great Britain.

FORCED CONVECTIVE HEAT TRANSFER IN A CURVED CHANNEL WITH A SQUARE CROSS SECTION

Y. MORI, Y. UCHIDA and T. UKON
Tokyo Institute of Technology, Onokayama, Meguro-ku, Tokyo, Japan

(*Received* 15 *October* 1970)

Abstract—Analytical and experimental results for a fully developed laminar flow in a curved channel with a square cross section are obtained under the condition of a constant wall heat flux. A secondary flow due to the centrifugal force appears in the channel, and the flow and the temperature fields are strongly influenced. In the case of an intense secondary flow, the concept of the boundary layer of the secondary flow is introduced. The moment and the energy equations in the boundary layer are solved on the basis of kinetic energy and entropy production balance. The resistance coefficient and the Nusselt number are obtained analytically and experimentally and it is shown that they are in good agreement.

NOMENCLATURE

C_1,	y-directional velocity component in the core region;
C_2,	$U_m(y = 0, z = 0)$;
C_3,	$T_m(y = 0, z = 0)$;
C_p,	specific heat at constant pressure;
d,	side length of the cross section;
k,	heat conductivity;
K,	Dean number, $Re\sqrt{d/R}$;
Nu,	Nusselt number, $qd/k\Delta T$;
P',	pressure;
P,	$P = P'/\rho\bar{U}^2$;
Pr,	Prandtl number, $\rho\nu C_p/k$;
q,	heat flux at the wall;
R,	radius of curvature of the channel;
Re,	Reynolds number, $\bar{U}d/\nu$;
T,	fluid temperature;
T,	$(T_w - T)/\tau d$;
T_w,	wall temperature;
ΔT,	temperature difference between the wall temperature and the mixed mean fluid temperature;
(U, V, W),	velocity component in the (θ, Y, Z)-direction;
$\bar{U}$,	mean velocity in the θ-direction;
(u, v, w),	$(U, V, W)/\bar{U}$;
(θ, Y, Z),	co-ordinate system (see Fig. 1);
(y, z),	$(Y, Z)/d$.

Greek symbols

δ,	non-dimensional velocity boundary layer thickness (non-dimensionized by d);
δ_T,	non-dimensional temperature boundary layer thickness;
η,	$\eta = 1/2 - \lvert y \rvert$;
ξ,	$\xi = 1/2 - \lvert z \rvert$;
ζ,	$\zeta = \delta_T/\delta$;
τ,	wall temperature gradient (constant);
λ,	resistance coefficient, $\partial P/(R/d) . \partial\theta$;
ρ,	density;
ν,	kinematic viscosity.

Subscripts

m,	core region;
i, ii, iii, iv, v,	characteristic region in the boundary layer along the wall;
0,	straight channel.

1. INTRODUCTION

CURVED channels with rectangular cross sections are widely used for heat exchange and cooling in many industrial fields, for example, cooling of hollow conductors in cryogenic engineering and it is important to obtain basic knowledge about their performance in heat transfer. In this report, the analytical and the experimental results for a laminar flow and temperature fields in a curved channel, of a square cross section, are presented. In a flow in a curved channel, centrifugal force acts on a fluid as a body force and a secondary flow is caused by this body force. The flow and the temperature fields are seriously affected by this secondary flow.

Many experimental [1, 2] and analytical results [3] on pressure loss and heat transfer for a flow in a curved circular pipe have already been published. The momentum and energy equations in a boundary layer of the secondary flow, which exists along the wall of the curved pipe, were used to analyze the flow and the temperature fields. However, it is difficult to use the same method to analyze the flow and the temperature fields in a square curved channel.

At the central part of the flow passage, when the intensity of the secondary flow is strong, it is possible to neglect the affect of the viscosity and heat conduction compared with a stress analogous to the Reynolds stress and heat convection due to the secondary flow components. The affect of the viscosity and heat conduction are confined within a thin layer along a wall of the passage, where the intensity of the secondary flow is weakened. Because of this, we can consider the existence of the boundary layer along the wall of the passage for a flow which is strongly affected by the secondary flow. In the following analysis, the flow and temperature fields in the curved channel are divided into two regions, that is, the core region about the central part of the passage where the affect of the secondary flow is dominant over the viscosity and heat conduction and the boundary layer region along the wall where the affect of the viscosity and heat conduction cannot be ignored. The existence of such a boundary layer is confirmed by experimental results. The kinetic energy and entropy production balance equations in the boundary layer, which are obtained by use of momentum and energy equations, are used to solve the flow and the temperature fields. This method has a wide applicability and can be applied to a flow in a channel which has a non-circular cross section.

2. ANALYSIS

2.1. *Analysis of the velocity field*

The following analysis is valid for a fully developed laminar flow in a square cross sectional curved channel, whose wall temperature gradient is kept constant. All physical properties are assumed to be constant.

As we assume that physical properties are constant, the velocity and the temperature fields are independent and we can solve the temperature field by using the results of the velocity field.

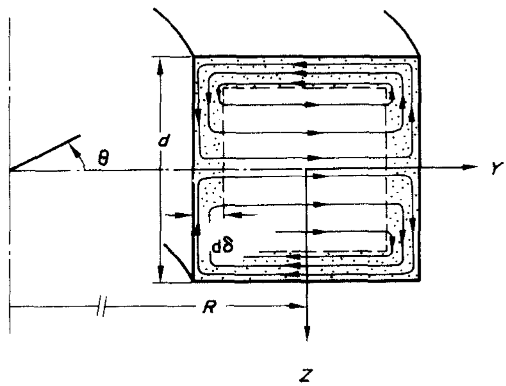

FIG. 1. The co-ordinate system.

As is indicated in Fig. 1, for a flow in a curved channel, the secondary flow, which consists of a pair of longitudinal vortex rolls, appears in the passage due to the affect of the centrifugal force. The intensity of the secondary flow depends upon the value of the Dean number $K(K = Re\sqrt{d/R})$. In the case of a small Dean number, the intensity of the secondary flow is weak and the affect of the viscosity must be considered in the whole cross section of the channel. The dissipation of the kinetic energy due to the viscosity cannot be neglected in the core.

With the increase of the Dean number, the intensity of the secondary flow becomes strong. For such a state, the affect of the viscosity can be distinguished only in a thin layer along the wall and it is possible to neglect its influence in the core. Therefore, we consider the existence of the boundary layer and assume that the effect of the viscosity is confined in that layer.

As is indicated above, for the flow with an intensive secondary flow, it is possible to consider two different regions; the core region and the boundary layer region. In the following sections, we analyze each region and obtain the solution for the flow field.

2.1.1. *Velocity distribution in the core region.* Indicating the values in the core region by suffix m, and neglecting the terms that indicate the effect of the viscosity, we obtain the following equations for the core region:

$$v_m \frac{\partial v_m}{\partial y} + w_m \frac{\partial v_m}{\partial z} - \frac{u_m^2}{(R/d)} = -\frac{\partial P_m}{\partial y} \tag{1}$$

$$v_m \frac{\partial u_m}{\partial y} + w_m \frac{\partial u_m}{\partial z} = \lambda \tag{2}$$

$$v_m \frac{\partial w_m}{\partial y} + w_m \frac{\partial w_m}{\partial z} = -\frac{\partial P_m}{\partial z} \tag{3}$$

$$\frac{\partial v_m}{\partial y} + \frac{\partial w_m}{\partial z} = 0 \tag{4}$$

where the higher order terms of d/R are neglected in the consideration of the fact of $d/R \ll 1$.

Equations (1)–(3) are the momentum equations and equation (4) is the continuity equation. The particular solution for the above equations is obtained if we assume that the secondary flow in the core region can be expressed by a uniform stream which flows from the inner to the outer part of the curvature. The velocity components in the y–z plane for such a uniform stream are given as $v_m = C_1$ (C_1 is constant) and $w_m = 0$. Substituting these relations into equations (1) and (2), we can solve u_m and P_m. The results are given in the following equations.

$$v_m = C_1 \tag{5}$$

$$u_m(y) = C_2 + \frac{\lambda}{C_1} y \tag{6}$$

$$w_m = 0 \tag{7}$$

$$P_m(y) = -\frac{R}{d}\lambda\theta + \left(C_2 + \frac{\lambda}{C_1} y\right)^3 \frac{1}{3(R/d)} \frac{C_1}{\lambda} + P_\delta \tag{8}$$

where C_2 and p_δ are constant.

2.1.2. *The kinetic energy balance in the boundary layer.* On the assumption that a velocity boundary layer of a constant thickness δ exists along the wall, we obtain the relations that indicate the balance of the kinetic energy inside the boundary layer. Error caused by this assumption might be serious near the point where the secondary flow separates from the wall ($y = \frac{1}{2}$, $z = 0$), but this local error can be neglected in the calculation of the resistance coefficient.

We divide the velocity boundary layer along the wall into five characteristic regions as shown in Fig. 2 and have the boundary layer equations in each region considering the fact of $d/R \ll 1$.

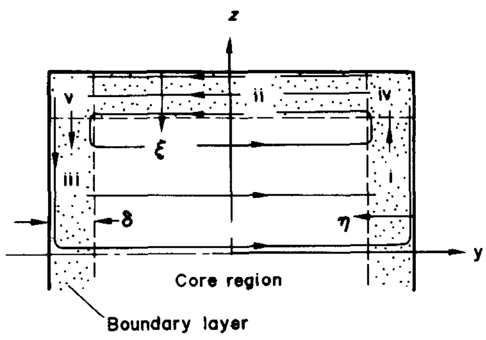

FIG. 2. The velocity boundary layer along the wall.

Equations in region i are ($\eta = \frac{1}{2} - y$)

$$\frac{\partial P}{\partial \eta} + \frac{u^2}{(R/d)} + \frac{1}{Re}\frac{\partial^2 v}{\partial \eta^2} = 0 \tag{9}$$

$$\lambda + v\frac{\partial u}{\partial \eta} - w\frac{\partial u}{\partial z} + \frac{1}{Re}\frac{\partial^2 u}{\partial \eta^2} = 0 \quad (10)$$

$$-\frac{\partial P}{\partial z} + v\frac{\partial w}{\partial \eta} - w\frac{\partial w}{\partial z} + \frac{1}{Re}\frac{\partial^2 w}{\partial \eta^2} \quad (11)$$

$$-\frac{\partial v}{\partial \eta} + \frac{\partial w}{\partial z} = 0. \quad (12)$$

Equations in region ii are ($\xi = \frac{1}{2} - z$)

$$-\frac{\partial P}{\partial y} - v\frac{\partial v}{\partial y} + w\frac{\partial v}{\partial \xi} + \frac{u^2}{(R/d)} + \frac{1}{Re}\frac{\partial^2 v}{\partial \xi^2} = 0 \quad (13)$$

$$\lambda - v\frac{\partial u}{\partial y} + w\frac{\partial u}{\partial \xi} + \frac{1}{Re}\frac{\partial^2 u}{\partial \xi^2} = 0 \quad (14)$$

$$\frac{\partial P}{\partial \xi} - v\frac{\partial w}{\partial y} + w\frac{\partial w}{\partial \xi} + \frac{1}{Re}\frac{\partial^2 w}{\partial \xi^2} = 0 \quad (15)$$

$$\frac{\partial v}{\partial y} - \frac{\partial w}{\partial \xi} = 0. \quad (16)$$

Equations in region iii are ($\eta = \frac{1}{2} + y$)

$$-\frac{\partial P}{\partial \eta} + \frac{u^2}{(R/d)} + \frac{1}{Re}\frac{\partial^2 v}{\partial \eta^2} = 0 \quad (17)$$

$$\lambda - v\frac{\partial u}{\partial \eta} - w\frac{\partial u}{\partial z} + \frac{1}{Re}\frac{\partial^2 u}{\partial \eta^2} = 0 \quad (18)$$

$$-\frac{\partial P}{\partial z} - v\frac{\partial w}{\partial \eta} - w\frac{\partial w}{\partial z} + \frac{1}{Re}\frac{\partial^2 w}{\partial \eta^2} = 0 \quad (19)$$

$$\frac{\partial v}{\partial \eta} + \frac{\partial w}{\partial z} = 0. \quad (20)$$

Equations in region iv are ($\eta = \frac{1}{2} - y$, $\xi = \frac{1}{2} - z$)

$$\frac{\partial P}{\partial \eta} + v\frac{\partial v}{\partial \eta} + w\frac{\partial v}{\partial \xi} + \frac{1}{Re}\left(\frac{\partial^2 v}{\partial \eta^2} + \frac{\partial^2 v}{\partial \xi^2}\right) = 0 \quad (21)$$

$$\lambda + v\frac{\partial u}{\partial \eta} + w\frac{\partial u}{\partial \xi} + \frac{1}{Re}\left(\frac{\partial^2 u}{\partial \eta^2} + \frac{\partial^2 u}{\partial \xi^2}\right) = 0 \quad (22)$$

$$\frac{\partial P}{\partial \xi} + v\frac{\partial w}{\partial \eta} + w\frac{\partial w}{\partial \xi} + \frac{1}{Re}\left(\frac{\partial^2 w}{\partial \eta^2} + \frac{\partial^2 w}{\partial \xi^2}\right) = 0 \quad (23)$$

$$\frac{\partial v}{\partial \eta} + \frac{\partial w}{\partial \xi} = 0. \quad (24)$$

Equations in region v are ($\eta = \frac{1}{2} + y$, $\xi = \frac{1}{2} - z$)

$$-\frac{\partial P}{\partial \eta} - v\frac{\partial v}{\partial \eta} + w\frac{\partial v}{\partial \xi} + \frac{1}{Re}\left(\frac{\partial^2 v}{\partial \eta^2} + \frac{\partial^2 v}{\partial \xi^2}\right) = 0 \quad (25)$$

$$\lambda - v\frac{\partial u}{\partial \eta} + w\frac{\partial u}{\partial \xi} + \frac{1}{Re}\left(\frac{\partial^2 u}{\partial \eta^2} + \frac{\partial^2 u}{\partial \xi^2}\right) = 0 \quad (26)$$

$$\frac{\partial P}{\partial \xi} - v\frac{\partial w}{\partial \eta} + w\frac{\partial w}{\partial \xi} + \frac{1}{Re}\left(\frac{\partial^2 w}{\partial \eta^2} + \frac{\partial^2 w}{\partial \xi^2}\right) = 0 \quad (27)$$

$$\frac{\partial v}{\partial \eta} - \frac{\partial w}{\partial \xi} = 0. \quad (28)$$

To obtain the kinetic energy balance equations, the momentum equations in each region are multiplied by the corresponding velocity components and then each equation is integrated over its region. Adding the kinetic energy balance equations in each region, we obtain the equation which indicates the kinetic energy balance in the whole region of the boundary layer along the wall.

The kinetic energy balance equation in the y–z plane becomes:

$$\int_0^{\frac{1}{2}-\delta} \{[v_{\mathrm{i}}P_{\mathrm{i}}]_{\eta=\delta} - [v_{\mathrm{iii}}P_{\mathrm{iii}}]_{\eta=\delta}\}\,\mathrm{d}z + \int_0^{\delta}\int_0^{\frac{1}{2}-\delta}\left(\frac{u^2 v}{R/d} + vw\frac{\partial w}{\partial \eta} - w^2\frac{\partial w}{\partial z}\right)_{\mathrm{i}}\mathrm{d}\eta\,\mathrm{d}z$$

$$+ \frac{1}{Re}\int_0^{\delta}\int_0^{\frac{1}{2}-\delta}\left(v\frac{\partial^2 v}{\partial \eta^2} + w\frac{\partial^2 w}{\partial \eta^2}\right)_{\mathrm{i}}\mathrm{d}\eta\,\mathrm{d}z + \int_0^{\delta}\int_0^{\delta}\left(v^2\frac{\partial v}{\partial \eta} + vw\frac{\partial v}{\partial \xi} + vw\frac{\partial w}{\partial \eta} + w^2\frac{\partial w}{\partial \xi}\right)_{\mathrm{iv}}\mathrm{d}\eta\,\mathrm{d}\xi$$

$$+\frac{1}{\boldsymbol{Re}}\int_0^{\delta}\int_0^{\delta}\left(\boldsymbol{v}\frac{\boldsymbol{\partial^2 v}}{\boldsymbol{\partial\eta^2}}+\boldsymbol{v}\frac{\boldsymbol{\partial^2 v}}{\boldsymbol{\partial\xi^2}}+\boldsymbol{w}\frac{\boldsymbol{\partial^2 w}}{\boldsymbol{\partial\eta^2}}+\boldsymbol{w}\frac{\boldsymbol{\partial^2 w}}{\boldsymbol{\partial\xi^2}}\right)_{\mathrm{iv}}\mathrm{d}\eta\,\mathrm{d}\xi+\int_{-\frac{1}{2}+\delta}^{\frac{1}{2}-\delta}\int_0^{\delta}\left(-v^2\frac{\partial v}{\partial y}+vw\frac{\partial v}{\partial\xi}-\boldsymbol{vw}\frac{\boldsymbol{\partial w}}{\boldsymbol{\partial y}}\right.$$

$$\left.+\boldsymbol{w^2}\frac{\boldsymbol{\partial w}}{\boldsymbol{\partial\xi}}+\frac{u^2v}{R/d}\right)_{\mathrm{ii}}\mathrm{d}y\,\mathrm{d}\xi+\frac{1}{Re}\int_{-\frac{1}{2}+\delta}^{\frac{1}{2}-\delta}\int_0^{\delta}\left(v\frac{\partial^2 v}{\partial\xi^2}+\boldsymbol{w}\frac{\boldsymbol{\partial^2 w}}{\boldsymbol{\partial\xi^2}}\right)_{\mathrm{ii}}\mathrm{d}y\,\mathrm{d}\xi+\int_0^{\delta}\int_0^{\delta}\left(-v^2\frac{\partial v}{\partial\eta}+vw\frac{\partial v}{\partial\xi}\right.$$

$$\left.-vw\frac{\partial w}{\partial\eta}+w^2\frac{\partial w}{\partial\xi}\right)_{\mathrm{v}}\mathrm{d}\eta\,\mathrm{d}\xi+\frac{1}{\boldsymbol{Re}}\int_0^{\delta}\int_0^{\delta}\left(\boldsymbol{v}\frac{\boldsymbol{\partial^2 v}}{\boldsymbol{\partial\eta^2}}+\boldsymbol{v}\frac{\boldsymbol{\partial^2 v}}{\boldsymbol{\partial\xi^2}}+\boldsymbol{w}\frac{\boldsymbol{\partial^2 w}}{\boldsymbol{\partial\eta^2}}+\boldsymbol{w}\frac{\boldsymbol{\partial^2 w}}{\boldsymbol{\partial\xi^2}}\right)_{\mathrm{v}}\mathrm{d}\eta\,\mathrm{d}\xi$$

$$+\int_0^{\delta}\int_0^{\frac{1}{2}-\delta}\left(\frac{\boldsymbol{u^2v}}{\boldsymbol{R/d}}-vw\frac{\partial w}{\partial\eta}-w^2\frac{\partial w}{\partial z}\right)_{\mathrm{iii}}\mathrm{d}\eta\,\mathrm{d}z+\frac{1}{Re}\int_0^{\delta}\int_0^{\frac{1}{2}-\delta}\left(\boldsymbol{v}\frac{\boldsymbol{\partial^2 v}}{\boldsymbol{\partial\eta^2}}+w\frac{\partial^2 w}{\partial\eta^2}\right)_{\mathrm{iii}}\mathrm{d}\eta\,\mathrm{d}z=0 \qquad (29)$$

The subscripts i, ii, iii, iv and v in the above equation indicate the values in the region i, ii, iii, iv and v, respectively. Terms set in bold type are the higher order terms of δ (δ is the non-dimensional thickness of the velocity boundary layer) compared with the other terms and can be neglected. The terms that indicate the dissipation energy in the region iv and v are also to be neglected, because the order of magnitude of these terms are δ^2.

The second term on the left side of equation (29) indicates the kinetic energy that is needed to accelerate the fluid in region i and the tenth term indicates the kinetic energy produced by the deceleration of the fluid in region iii. As the cross section of the passage and the flow pattern are symmetrical around the z-axis, the summation of these terms is reduced to zero. The summation of the fourth and the eighth term on the left hand side of equation (29) is also reduced to zero for the same reason.

Based on the above consideration, equation (29) is reduced to equation (30).

$$\int_0^{\frac{1}{2}-\delta} C_1\{P_m(\tfrac{1}{2}-\delta)-P_m(-\tfrac{1}{2}+\delta)\}\,\mathrm{d}z$$

$$+\int_{-\frac{1}{2}+\delta}^{\frac{1}{2}-\delta}\int_0^{\delta}\{u^2v/(R/d)\}_{\mathrm{ii}}\,\mathrm{d}y\,\mathrm{d}\xi$$

$$+\left[\frac{1}{Re}\int_0^{\delta}\int_0^{\frac{1}{2}-\delta}\left\{\left(w\frac{\partial^2 w}{\partial\eta^2}\right)_{\mathrm{i}}+\left(w\frac{\partial^2 w}{\partial\eta^2}\right)_{\mathrm{iii}}\right\}\mathrm{d}\eta\,\mathrm{d}z\right.$$

$$\left.+\int_{-\frac{1}{2}+\delta}^{\frac{1}{2}-\delta}\int_0^{\delta}\left(v\frac{\partial^2 v}{\partial\xi^2}\right)_{\mathrm{ii}}\mathrm{d}y\,\mathrm{d}\xi\right]=0. \qquad (30)$$

The first term on the left side of equation (30) represents the kinetic energy introduced into the boundary layer from the core region due to pressure; the second term represents the energy that is required to make the fluid flow in region against the centrifugal force; the third term represents the energy dissipated by the viscosity. Equation (30) indicates that the secondary flow is maintained by such a simple energy balance mechanism that it absorbs the kinetic energy from the core region and loses that energy because of the body force and the viscosity.

The kinetic energy balance equation in the flow direction (θ-direction) becomes:

$$\lambda\left[\int_0^{\delta}\int_0^{\frac{1}{2}-\delta}u_{\mathrm{i}}\,\mathrm{d}\eta\,\mathrm{d}z+\int_0^{\delta}\int_0^{\delta}u_{\mathrm{iv}}\,\mathrm{d}\eta\,\mathrm{d}\xi+\int_{-\frac{1}{2}+\delta}^{\frac{1}{2}+\delta}\int_0^{\delta}u_{\mathrm{ii}}\,\mathrm{d}y\,\mathrm{d}\xi+\int_0^{\delta}\int_0^{\delta}u_{\mathrm{v}}\,\mathrm{d}\eta\,\mathrm{d}\xi+\int_0^{\delta}\int_0^{\frac{1}{2}-\delta}u_{\mathrm{iii}}\,\mathrm{d}\eta\,\mathrm{d}z\right]$$

$$+\int_0^{\delta}\int_0^{\frac{1}{2}-\delta}\left(uv\frac{\partial u}{\partial \eta}-uw\frac{\partial u}{\partial z}\right)_{\mathrm{i}}\mathrm{d}\eta\,\mathrm{d}z+\frac{1}{Re}\int_0^{\delta}\int_0^{\frac{1}{2}-\delta}\left(u\frac{\partial^2 u}{\partial \eta^2}\right)_{\mathrm{i}}\mathrm{d}\eta\,\mathrm{d}z$$

$$+\int_0^{\delta}\int_0^{\delta}\left(uv\frac{\partial u}{\partial \eta}+uw\frac{\partial u}{\partial \xi}\right)_{\mathrm{iv}}\mathrm{d}\eta\,\mathrm{d}\xi+\frac{1}{Re}\int_0^{\delta}\int_0^{\delta}\left(u\frac{\partial^2 u}{\partial \eta^2}+u\frac{\partial^2 u}{\partial \xi^2}\right)_{\mathrm{iv}}\mathrm{d}\eta\,\mathrm{d}\xi$$

$$+\int_{-\frac{1}{2}+\delta}^{\frac{1}{2}-\delta}\int_0^{\delta}\left(-uv\frac{\partial u}{\partial y}+uw\frac{\partial u}{\partial \xi}\right)_{\mathrm{ii}}\mathrm{d}y\,\mathrm{d}\xi+\frac{1}{Re}\int_{-\frac{1}{2}+\delta}^{-\frac{1}{2}+\delta}\int_0^{\delta}\left(u\frac{\partial^2 u}{\partial \xi^2}\right)_{\mathrm{ii}}\mathrm{d}u\,\mathrm{d}\xi$$

$$+\int_0^{\delta}\int_0^{\delta}\left(-uv\frac{\partial u}{\partial \eta}+uw\frac{\partial u}{\partial \xi}\right)_{\mathrm{v}}\mathrm{d}\eta\,\mathrm{d}\xi+\frac{1}{Re}\int_0^{\delta}\int_0^{\delta}\left(u\frac{\partial^2 u}{\partial \eta^2}+u\frac{\partial^2 u}{\partial \xi^2}\right)_{\mathrm{v}}\mathrm{d}\eta\,\mathrm{d}\xi$$

$$+\int_0^{\delta}\int_0^{\frac{1}{2}-\delta}\left(-uv\frac{\partial u}{\partial \eta}-uw\frac{\partial u}{\partial z}\right)_{\mathrm{iii}}\mathrm{d}\eta\,\mathrm{d}z+\frac{1}{Re}\int_0^{\delta}\int_0^{\frac{1}{2}-\delta}\left(u\frac{\partial^2 u}{\partial \eta^2}\right)_{\mathrm{iii}}\mathrm{d}\eta\,\mathrm{d}z=0. \quad (31)$$

Here, it must be mentioned that the following two relations are valid in regions iv and v, respectively.

$$\lambda\int_0^{\delta}\int_0^{\delta}u_{\mathrm{iv}}\,\mathrm{d}\eta\,\mathrm{d}\xi+\int_0^{\delta}\int_0^{\delta}\left(uv\frac{\partial u}{\partial \eta}+uw\frac{\partial u}{\partial \xi}\right)_{\mathrm{iv}}\mathrm{d}\eta\,\mathrm{d}\xi+\frac{1}{Re}\int_0^{\delta}\int_0^{\delta}\left(u\frac{\partial^2 u}{\partial \eta^2}+u\frac{\partial^2 u}{\partial \xi^2}\right)_{\mathrm{iv}}\mathrm{d}\eta\,\mathrm{d}\xi=0$$

$$\lambda\int_0^{\delta}\int_0^{\delta}u_{\mathrm{v}}\,\mathrm{d}\eta\,\mathrm{d}\xi+\int_0^{\delta}\int_0^{\delta}\left(-uv\frac{\partial u}{\partial \eta}+uw\frac{\partial u}{\partial \xi}\right)_{\mathrm{v}}\mathrm{d}\eta\,\mathrm{d}\xi+\frac{1}{Re}\int_0^{\delta}\int_0^{\delta}\left(u\frac{\partial^2 u}{\partial \eta^2}+u\frac{\partial^2 u}{\partial \xi^2}\right)_{\mathrm{v}}\mathrm{d}\eta\,\mathrm{d}\xi=0.$$

And as the cross section is symmetrical about the z-axis, the relation of $w_{\mathrm{i}} = -w_{\mathrm{iii}}$ must be considered.

Equation (31) is simplified to equation (32) by using these relations.

$$\lambda\left[\int_0^{\delta}\int_0^{\frac{1}{2}-\delta}\{u_{\mathrm{i}}+u_{\mathrm{iii}}\}\,\mathrm{d}\eta\,\mathrm{d}z+\int_{-\frac{1}{2}+\delta}^{\frac{1}{2}-\delta}\int_0^{\delta}u_{\mathrm{ii}}\,\mathrm{d}y\,\mathrm{d}\xi\right]$$

$$\int_0^{\delta}\int_0^{\frac{1}{2}-\delta}\left\{\left(uv\frac{\partial u}{\partial \eta}\right)_{\mathrm{i}}-\left(uv\frac{\partial u}{\partial \eta}\right)_{\mathrm{iii}}\right\}\mathrm{d}\eta\,\mathrm{d}z+\int_{-\frac{1}{2}+\delta}^{\frac{1}{2}-\delta}\int_0^{\delta}\left(-uv\frac{\partial u}{\partial y}\right)_{\mathrm{ii}}\mathrm{d}y\,\mathrm{d}\xi$$

$$+\frac{1}{Re}\left[\int_0^{\delta}\int_0^{\frac{1}{2}-\delta}\left\{\left(u\frac{\partial^2 u}{\partial \eta^2}\right)_{\mathrm{i}}+\left(u\frac{\partial^2 u}{\partial \eta^2}\right)_{\mathrm{iii}}\right\}\mathrm{d}\eta\,\mathrm{d}z+\int_{-\frac{1}{2}+\delta}^{\frac{1}{2}-\delta}\int_0^{\delta}\left(u\frac{\partial^2 u}{\partial \xi^2}\right)_{\mathrm{ii}}\mathrm{d}y\,\mathrm{d}\xi\right]=0. \quad (32)$$

The first term on the left side of equation (32) represents the kinetic energy from the pressure gradient in the θ-direction. The second term indicates that the work done by the pressure gradient in the core region is introduced into the boundary layer by means of $-uv$. The third term represents the energy dissipated by the viscosity.

The condition for the constant flow rate is written as follows:

$$\frac{1}{2} = \int_0^{\delta}\int_0^{\frac{1}{2}-\delta} \{u_{\mathrm{i}} + u_{\mathrm{iii}}\}\,\mathrm{d}\eta\,\mathrm{d}z + \int_{-\frac{1}{2}+\delta}^{\frac{1}{2}-\delta}\int_0^{\delta} u_{\mathrm{ii}}\,\mathrm{d}y\,\mathrm{d}\xi + \int_{-\frac{1}{2}+\delta}^{\frac{1}{2}-\delta}\int_0^{\frac{1}{2}-\delta} u_m(y)\,\mathrm{d}y\,\mathrm{d}z. \tag{33}$$

The first and the second terms on the right hand side of equation (33) represent the flow rate in the boundary layer, and the third term is the flow rate in the core region. The flow rate in regions iv and v can be neglected because their orders of magnitude are δ^2.

Considering the balance of force between two cross sections in the axial direction, the distance between them being $(R/d)\mathrm{d}\theta$, we obtain equation (34).

$$\frac{\lambda}{2} = \frac{1}{Re}\left[\int_0^{\frac{1}{2}-\delta}\left\{\left(\frac{\partial u_{\mathrm{i}}}{\partial\eta}\right)_{\eta=0} + \left(\frac{\partial u_{\mathrm{iii}}}{\partial\eta}\right)_{\eta=0}\right\}\mathrm{d}z + \int_{\frac{1}{2}-\delta}^{\frac{1}{2}}\left\{\left(\frac{\partial u_{\mathrm{iv}}}{\partial\eta}\right)_{\eta=0} + \left(\frac{\partial u_{\mathrm{v}}}{\partial\eta}\right)_{\eta=0}\right\}\mathrm{d}z + \int_0^{\delta}\left\{\left(\frac{\partial u_{\mathrm{iv}}}{\partial\xi}\right)_{\xi=0} + \left(\frac{\partial u_{\mathrm{v}}}{\partial\xi}\right)_{\xi=0}\right\}\mathrm{d}\eta + \int_{-\frac{1}{2}+\delta}^{\frac{1}{2}-\delta}\left(\frac{\partial u_{\mathrm{ii}}}{\partial\xi}\right)_{\xi=0}\mathrm{d}y\right]. \tag{34}$$

The left hand term of the above equation represents the pressure drop, and the right hand term the shear stress at the wall surface.

Four unknowns exist; C_1, C_2, λ and δ C_1 and C_2 indicate the intensity of the secondary flow in the core region and the value of the θ-directional velocity component at the center of the passage, respectively. λ is the resistance coefficient and δ is the non-dimensional thickness of the velocity boundary layer. If the velocity distributions in regions i, ii and iii are known, these unknowns are solved by use of equations (30), (32), (33) and (34).

2.1.3. *The velocity distribution in the boundary layer.* (i) The velocity distribution in region i. We consider a rectangle ABCD in region i as shown in Fig. 3. The flow rate of the secondary

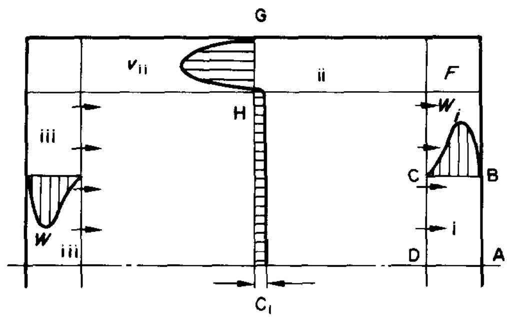

FIG. 3. The velocity distribution in the boundary layer.

flow that flows into the boundary layer through the boundary CD must cross the BC plane. Because of the continuity of the flow rate of the secondary flow, we have the following equation:

$$C_1 z = \int_0^{\delta} w_{\mathrm{i}}\,\mathrm{d}\eta. \tag{35}$$

Boundary conditions for w_{i} are given by equation (36).

$$\left.\begin{aligned} w_{\mathrm{i}} &= 0 && \text{at} \quad \eta = 0 \\ w_{\mathrm{i}} &= \frac{\partial w_{\mathrm{i}}}{\partial\eta} = 0 && \text{at} \quad \eta = \delta. \end{aligned}\right\} \tag{36}$$

Equation (36) indicates that w_{i} must reduce to zero at the wall surface. At the edge of the boundary layer, w_{i} and its gradient are smoothly connected with their values in the core region. Here we assume that the distribution of w_{i} can be expressed by a polynomial of η, that satisfies equations (35) and (36), as follows:

$$w_i = \frac{12}{\delta} C_1 z \left\{ \left(\frac{\eta}{\delta}\right) - 2\left(\frac{\eta}{\delta}\right)^2 + \left(\frac{\eta}{\delta}\right)^3 \right\}. \quad (37)$$

By use of equation (37) and the continuity equation of $-\partial v_i/\partial \eta + \partial w_i/\partial z = 0$, we obtain the distribution of v_i.

$$v_i = \frac{12}{\delta} C_1 \left\{ \frac{1}{2\delta}\eta^2 - \frac{2}{3\delta^2}\eta^3 + \frac{1\eta^4}{4\delta^3} \right\}. \quad (38)$$

This distribution satisfies the condition at the edge of the boundary layer that v_i and its gradient smoothly connect with the core region distribution, $v_m = C_1$.

The distribution of u_i is expressed by equation (40) so as to satisfy the boundary conditions given by equation (39).

$$u_i = 0 \quad \text{at} \quad \eta = 0, \qquad u_i = u_m(\tfrac{1}{2} - \delta),$$

$$\frac{\partial u_i}{\partial \eta} = -\left.\frac{\mathrm{d}u_m}{\mathrm{d}y}\right|_{y=\frac{1}{2}-\delta} \quad \text{at} \quad \eta = \delta \quad (39)$$

$$u_i = \left\{ -\frac{\lambda}{C_1} + \frac{2}{\delta}\left(C_2 + \frac{\lambda}{2C_1}\right) \right\} \times \eta - \frac{1}{\delta^2}\left(C_2 + \frac{\lambda}{2C_1}\right)\eta^2. \quad (40)$$

(ii) The velocity distribution in region ii. As we assumed that the thickness of the boundary layer was constant, the flow rate of the secondary flow that flows into the boundary layer through the plane DF (see Fig. 3) should pass over the plane GH. This condition is expressed by equation (41).

$$(\tfrac{1}{2} - \delta) C_1 = \int_0^\delta (-v_{ii})\, \mathrm{d}\xi. \quad (41)$$

The distribution of v_{ii} that satisfies equations (41) and (42) is given by equation (43).

$$v_{ii} = 0 \quad \text{at} \quad \xi = 0,$$

$$v_{ii} = C_1, \ \frac{\partial v_{ii}}{\partial \xi} = 0 \quad \text{at} \quad \xi = \delta \quad (42)$$

$$v_{ii} = \frac{C_1}{\delta^2}(6\delta - 6)\xi + \frac{C_1}{\delta^3}(-9\delta + 12)\xi^2 + \frac{C_1}{\delta^4}(4\delta - 6)\xi^3. \quad (43)$$

The distribution of w_{ii} that satisfies the continuity equation of $\partial v_{ii}/\partial y - \partial w_{ii}/\partial \xi = 0$ and boundary conditions of $w_{ii} = 0$ at $\xi = 0, \delta$ is given by equation (44).

$$w_{ii} = 0. \quad (44)$$

Boundary conditions and the distribution of u_{ii} are given by equations (45) and (46).

$$u_{ii} = 0 \quad \text{at} \quad \xi = 0,$$

$$u_{ii} = u_m(v), \ \frac{\partial u_{ii}}{\partial \xi} = 0 \quad \text{at} \quad \xi = \delta \quad (45)$$

$$u_{ii} = \left(C_2 + \frac{\lambda}{C_1} y\right)\left\{2\left(\frac{\xi}{\delta}\right) - \left(\frac{\xi}{\delta}\right)^2\right\}. \quad (46)$$

(iii) The velocity distribution in region iii. From the continuity of the secondary flow, we obtain equation (47).

$$\int_0^\delta (-w_{iii})\, \mathrm{d}n = C_1 z. \quad (47)$$

The boundary conditions for w_{iii} are given by equation (36). From equations (47) and (36), the distribution of w_{iii} is obtained.

$$w_{iii} = -w_i = \frac{12}{\delta} C_1 z \left\{ -\left(\frac{\eta}{\delta}\right) + 2\left(\frac{\eta}{\delta}\right)^2 - \left(\frac{\eta}{\delta}\right)^3 \right\}. \quad (48)$$

We express the distribution of v_{iii} so that it satisfies the continuity equation of $\partial v_{iii}/\partial \eta + \partial w_{iii}/\partial z = 0$ as follows:

$$v_{iii} = v_i = \frac{12}{\delta} C_1 \left\{ \frac{1}{2\delta}\eta^2 - \frac{2}{3\delta^2}\eta^3 + \frac{1}{4\delta^3}\eta^4 \right\}. \quad (49)$$

The boundary conditions and the distribution of u_{iii} are given by equations (50) and (51).

$$u_{iii} = 0 \quad \text{at} \quad \eta = 0, \qquad u_{iii} = u_m(-\tfrac{1}{2} + \delta),$$
$$\frac{\partial u_{iii}}{\partial \eta} = \left.\frac{du_m}{dy}\right|_{y=-\frac{1}{2}+\delta} \quad \text{at} \quad \eta = \delta \qquad (50)$$

$$u_{iii} = \left\{\frac{\lambda}{C_1} + \frac{2}{\delta}\left(C_2 - \frac{\lambda}{2C_1}\right)\right\} \times \eta - \frac{1}{\delta^2}\left(C_2 - \frac{\lambda}{2C_1}\right)\eta^2. \qquad (51)$$

2.1.4. *Solution for* C_1, C_2, λ, δ. Substituting the velocity distributions given in section 2.1.3 into equations (30)–(34), we obtain the following relations:

$$\frac{C_1}{(R/d)}\left\{2C_2^2 + \frac{2}{3}\left(\frac{\lambda}{C_1}\right)^2\left(\frac{1}{2} - \delta\right)^2\right\} \times \left(\frac{41}{140} - \frac{17}{42}\delta\right) = \frac{C_1}{Re} \times \left\{\frac{C_1}{\delta^3}\frac{4}{5}(28\,\delta^2 - 37\,\delta + 16)\right\} \qquad (52)$$

$$\lambda C_2\left\{-\frac{43}{105}\,\delta + 1\right\} - \frac{1}{\delta Re}\frac{16}{3}C_2^2 = \frac{2}{\delta Re}\left(\frac{\lambda}{C_1}\right)^2\left\{\frac{4}{9}\delta^2 - \frac{17}{18}\delta + \frac{4}{9}\right\} \qquad (53)$$

$$\tfrac{1}{2} = (\tfrac{1}{2} - \delta)(1 + \tfrac{2}{3}\delta)\,C_2 \qquad (54)$$

$$\frac{\lambda}{2} = \frac{1}{Re}\frac{4}{\delta}C_2. \qquad (55)$$

In the above equations, equation (54) results from equation (33). As we neglected the terms that represented the flow rate in region iv and v in equation (33), instead of equation (54) we have

$$\tfrac{1}{2} = \tfrac{1}{2}(1 - \tfrac{4}{3}\delta)\,C_2. \qquad (56)$$

Equation (55) is based on equation (34), and in obtaining equation (55), the following approximate relations were used.

$$\int_{\frac{1}{2}-\delta}^{\frac{1}{2}}\left(\frac{\partial u_{iv}}{\partial \eta}\right)_{\eta=0} dz \doteqdot \left.\frac{\partial u_i}{\partial \eta}\right|_{\eta=0,\,z=\frac{1}{2}-\delta} .\,\delta,$$

$$\int_{\frac{1}{2}-\delta}^{\frac{1}{2}}\left(\frac{\partial u_{v}}{\partial \eta}\right)_{\eta=0} dz \doteqdot \left.\frac{\partial u_{iii}}{\partial \eta}\right|_{\eta=0,\,z=\frac{1}{2}-\delta} .\,\delta$$

$$\int_0^{\delta}\left(\frac{\partial u_{iv}}{\partial \xi}\right)_{\xi=0} d\eta \doteqdot \left.\frac{\partial u_{ii}}{\partial \xi}\right|_{\xi=0,\,y=\frac{1}{2}-\delta} .\,\delta,$$

$$\int_0^{\delta}\left(\frac{\partial u_{v}}{\partial \xi}\right)_{\xi=0} d\eta \doteqdot \left.\frac{\partial u_{ii}}{\partial \xi}\right|_{\xi=0,\,y=-\frac{1}{2}+\delta} .\,\delta.$$

Considering the fact of $K \gg 1$, we expand δ and C_1 as follows:

$$\delta = \delta^* K^{-\frac{1}{4}} + \delta^{**} K^{-1} + \ldots,$$
$$C_1 = \frac{1}{Re}\{C^* K^{\frac{1}{4}} + C^{**} + \ldots\} \qquad (57)$$

where C^*, C^{**} and δ^*, δ^{**} are the coefficients of expansion.

Substituting equations (55)–(57) into equation (52), and equating the terms of the same order for $K^{-\frac{1}{4}}$, we get:

$$\tfrac{41}{140}(2C^{*2}\delta^{*2} + \tfrac{32}{3})\,\delta^* = \tfrac{64}{5}C^{*3} \qquad (58)$$

$$\tfrac{41}{140}\delta^{**}(2C^{*2}\delta^{*2} + \tfrac{32}{3}) + \delta^*[\tfrac{41}{140}\{4C^*\delta^*(C^*\delta^{**} + C^{**}\delta^*) - \tfrac{128}{3}\delta^*\} - \tfrac{17}{42}\delta^*(2C^{*2}\delta^{*2} + \tfrac{32}{3})] = \tfrac{4}{5}(48C^{*2}C^{**} - \tfrac{239}{3}C^{*3}\delta^*). \qquad (59)$$

By means of the same procedure, substituting equations (55)–(57) into equation (53), we obtain equations (60) and (61).

$$\tfrac{8}{3}C^{*2}\delta^{*2} = \tfrac{512}{9} \qquad (60)$$

$$\tfrac{16}{3}C^*\delta^*(C^*\delta^{**} + C^{**}\delta^*) - \tfrac{43}{105}C^{*2}\delta^{*3} = -\tfrac{1088}{9}\delta^*. \qquad (61)$$

From equations (58) and (60), δ^* and C^* are solved as follows:

$$\delta^* = 2{\cdot}998, \qquad C^* = 1{\cdot}541. \qquad (62)$$

Substituting the above result into equations (55)–(57), we obtain the following results as the first approximation for C_1, C_2, λ and δ.

$$C_{11} = 1{\cdot}541\,K^{\frac{1}{4}}/Re \qquad (63)$$

$$C_{21} = 1{\cdot}0 \tag{64}$$

$$\lambda_1 = 2{\cdot}668\, K^{\frac{1}{2}}/Re \tag{65}$$

$$\delta_1 = 2{\cdot}998\, K^{-\frac{1}{2}}. \tag{66}$$

Substituting equation (62) into equations (59) and (61), we obtain the expansion coefficients δ^{**} and C^{**}.

$$\delta^{**} = -\,9{\cdot}385, \qquad C^{**} = 0{\cdot}2703. \tag{67}$$

Substituting equations (62) and (67) into equations (55)–(57), we obtain the following results as the second approximation for C_1, C_2, λ and δ.

$$C_{12} = \frac{1}{Re}\{1{\cdot}541\, K^{\frac{1}{2}} + 0{\cdot}2703\} \tag{68}$$

$$C_{22} = \frac{1}{1 - 3{\cdot}996\, K^{-\frac{1}{2}}} \tag{69}$$

$$\lambda_2 = \frac{\lambda_1}{1 - 7{\cdot}126\, K^{-\frac{1}{2}}} \tag{70}$$

$$\delta_2 = 2{\cdot}998\, K^{-\frac{1}{2}} - 9{\cdot}385\, K^{-1}. \tag{71}$$

We define the resistance coefficient for a straight channel as λ_0 and it is well known that λ_0 equals $28{\cdot}45/Re$ for a laminar flow. By non-dimensionizing λ_1 and λ_2 by λ_0, the values of λ_1 and λ_2 are given by equations (65) and (70), respectively, and we obtain the following results:

$$\frac{\lambda_1}{\lambda_0} = 0{\cdot}09378\, K^{\frac{1}{2}} \tag{72}$$

$$\frac{\lambda_2}{\lambda_0} = \frac{0{\cdot}09378\, K^{\frac{1}{2}}}{1 - 7{\cdot}126\, K^{-\frac{1}{2}}}. \tag{73}$$

2.2. *Analysis of the temperature field*

We consider a fully developed temperature field under the condition of a constant wall temperature gradient. The surface temperature of the wall is expressed as $T_w = \tau R\theta$, where τ is a wall temperature gradient. Neglecting the higher order terms of d/R, we can write the energy equation as follows:

$$v\frac{\partial T}{\partial y} - u + w\frac{\partial T}{\partial z} = \frac{1}{Pr\, Re}\left(\frac{\partial^2 T}{\partial y^2} + \frac{\partial^2 T}{\partial z^2}\right). \tag{74}$$

2.2.1. *The temperature distribution in the core region.* We divide the temperature field into two regions, the core and the thermal boundary region. In the core region, convective heat transfer due to the secondary flow components predominates, and the effect of heat conduction can be neglected. The effect of heat conduction must be considered only within the thermal boundary layer along the wall.

By substituting the velocity distributions in the core region, given by equations (5)–(7), into equation (74), and neglecting the conduction terms on the right hand side of that equation, we obtain the temperature distribution in the core region.

$$T_m(y) = C_3 + \frac{C_2}{C_1}y + \frac{\lambda}{2C_1^2}y^2. \tag{75}$$

In the above equation, C_3 is an unknown constant and C_1, C_2 and λ are given in equations (63–65).

2.2.2. *The entropy production balance in the thermal boundary layer.* We assume that a thermal boundary layer exists along the wall and the thickness of the layer, δ_T, is constant. Then we divide the thermal boundary layer into five characteristic regions as shown in Fig. 4

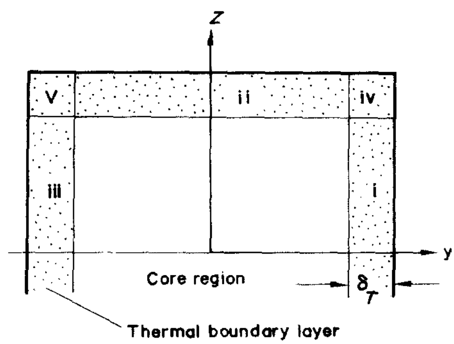

FIG. 4. The thermal boundary layer along the wall.

and consider the entropy production balance in each region. From the consideration on the order of magnitude, it is known that the entropy production in region iv and v can be neglected compared with those in the other regions. Therefore, we confine our analysis to regions i, ii and iii in the remainder of this section. It is also known from the consideration on the order of magnitude that the second term on the left hand side of equation (74), that indicates heat transfer due to temperature gradient in the flow direction, can be neglected compared with the other terms.

Based on the above consideration, we can write the energy equation in the thermal boundary layer as follows:

Equation in region i ($\eta = \frac{1}{2} - y$)

$$-v\frac{\partial T}{\partial \eta} + w\frac{\partial T}{\partial z} = \frac{1}{Pr\,Re}\frac{\partial^2 T}{\partial \eta^2}.$$

Equation in region ii ($\xi = \frac{1}{2} - z$)

$$v\frac{\partial T}{\partial y} - w\frac{\partial T}{\partial \xi} = \frac{1}{Pr\,Re}\frac{\partial^2 T}{\partial \xi^2}.$$

Equation in region iii ($\eta = \frac{1}{2} + y$)

$$v\frac{\partial T}{\partial \eta} + w\frac{\partial T}{\partial z} = \frac{1}{Pr\,Re}\frac{\partial^2 T}{\partial \eta^2}.$$

Multiplying each boundary layer equation by T and then integrating each region and adding these equations, we obtain the relation that indicates the balance of the entropy production in the thermal boundary layer.

$$\frac{1}{2}\int_0^{\frac{1}{2}-\delta} C_1\{T_m^2(\tfrac{1}{2}-\delta) - T_m^2(-\tfrac{1}{2}+\delta)\}\,dz$$
$$= -\frac{1}{Pr\,Re}\left[\int_0^{\delta}\int_0^{\frac{1}{2}-\delta}\left\{\left(T\frac{\partial^2 T}{\partial \eta^2}\right)_{i} + \left(T\frac{\partial^2 T}{\partial \eta^2}\right)_{iii}\right\}d\eta\,dz + \int_{-\frac{1}{2}+\delta}^{\frac{1}{2}-\delta}\int_0^{\delta}\left(T\frac{\partial^2 T}{\partial \xi^2}\right)_{ii} dy\,d\xi\right]. \quad (76)$$

The term on the left hand side represents the entropy production due to heat transfer caused by the secondary flow components and the term on the right hand side the entropy production due to heat conduction. Equation (76) indicates that these entropy productions balance each other in a steady state.

In the case of $\delta < \delta_T$, the integration in equation (76) must be performed from 0 to δ_T instead of 0–δ. But, since we neglect the higher order terms in the entropy production balance equation, it is still possible to use equation (76) even when δ_T is larger than δ.

Considering the heat balance between two cross sections, the distance between them being $(R/d)\,d\theta$, we obtain the following equation:

$$\frac{1}{2} = \frac{1}{Pr\,Re}\left[\int_0^{\frac{1}{2}-\delta}\left\{\left(\frac{\partial T_i}{\partial \eta}\right)_{\eta=0} + \left(\frac{\partial T_{iii}}{\partial \eta}\right)_{\eta=0}\right\}dz + \int_{-\frac{1}{2}+\delta}^{\frac{1}{2}-\delta}\left(\frac{\partial T_{ii}}{\partial \xi}\right)_{\xi=0} dy\right]. \quad (77)$$

The left term of equation (77) represents the temperature rise in the flow direction and the right term the heat flux at the wall.

Two equations for two unknowns exist, C_3 and δ_T; therefore, we can solve these if the temperature distribution in the thermal boundary layer is known. In the following section, we solve ζ, $\zeta = \delta_T/\delta$, instead of δ_T.

2.2.3. *The temperature distribution in the thermal boundary layer.* (i) The case of $\zeta \geqslant 1$. Since δ_T is larger than δ, the temperature distribution in the core region, given in equation (75), is valid at the edge of the thermal boundary layer. Therefore, we assume that the temperature distribution can be expressed by polynomials of η and ξ which satisfy the boundary conditions given at the wall and at the edge of the thermal boundary layer.

(a) The temperature distribution in region i.

Boundary conditions for T_i are given as follows:

$T_i = 0$ at $\eta = 0$, $\quad T_i = T_m(\frac{1}{2} - \delta_T)$,

$$\frac{\partial T_i}{\partial \eta} = -\left.\frac{\mathrm{d}T_m}{\mathrm{d}y}\right|_{y=\frac{1}{2}-\delta_T} \quad \text{at} \quad \eta = \delta_T.$$

The first condition means that T_i is reduced to zero at the wall and the second means that T_i and its gradient are smoothly connected with their values in the core region at the edge of the thermal boundary layer.

Considering the boundary conditions, we assume the distribution of T_i by a polynomial of η as follows:

$$T_i = T_m(\tfrac{1}{2} - \delta_T)\cdot\left\{2\frac{\eta}{\delta_T} - \left(\frac{\eta}{\delta_T}\right)^2\right\} + \delta_T\left\{\frac{C_2}{C_1} + \frac{\lambda}{C_1^2}\cdot(\tfrac{1}{2} - \delta_T)\right\} \times \left\{\left(\frac{\eta}{\delta_T}\right)^2 - \left(\frac{\eta}{\delta_T}\right)^3\right\} \quad (78)$$

(b) The temperature distribution in region ii.

Boundary conditions and the distribution of T_{ii} are given as follows:

Boundary conditions;

$$T_{ii} = 0 \quad \text{at} \quad \xi = 0,$$

$$T_{ii} = T_m(y), \quad \frac{\partial T_{ii}}{\partial \xi} = 0 \quad \text{at} \quad \xi = \delta_T.$$

Distribution of T_{ii};

$$T_{ii} = T_m(y)\cdot\left\{2\left(\frac{\xi}{\delta_T}\right) - \left(\frac{\xi}{\delta_T}\right)^2\right\}. \quad (79)$$

(c) The temperature distribution in region iii.

Boundary conditions and the distribution of T_{iii} are given as follows:

$$T_{iii} = 0 \quad \text{at} \quad \eta = 0, \qquad T_{iii} = T_m(-\tfrac{1}{2} + \delta_T),$$

$$\frac{\partial T_{iii}}{\partial \eta} = \left.\frac{\mathrm{d}T_m}{\mathrm{d}y}\right|_{y=-\frac{1}{2}+\delta_T} \quad \text{at} \quad \eta = \delta_T,$$

$$T_{iii} = T_m(-\tfrac{1}{2} + \delta_T)\left\{2\left(\frac{\eta}{\delta_T}\right) - \left(\frac{\eta}{\delta_T}\right)^2\right\} - \delta_T\left\{\frac{C_2}{C_1} - \frac{\lambda}{C_1^2}(\tfrac{1}{2} - \delta_T)\right\}\left\{\left(\frac{\eta}{\delta_T}\right)^2 - \left(\frac{\eta}{\delta_T}\right)^3\right\}. \quad (80)$$

(ii) The case of $\zeta \leqslant 1$.

As δ_T is smaller than δ, it is impossible to extend the temperature distribution in the core region to the outer edge of the thermal boundary layer. Boundary conditions for the temperature distribution are given at the edge of the velocity boundary layer and at the wall. Conditions at the edge of the velocity boundary layer are so given as the values of the temperature distribution and its gradient connect smoothly with their values in the core region. But at the wall, besides the condition of $T = 0$, we must consider another condition; that is, the temperature gradient must be the same magnitude as the value for the case of $\zeta \geqslant 1$.

(a) The temperature distribution in region i.

Boundary conditions and the distribution of T_i are given as follows:

$$T_i = 0, \qquad \frac{\partial T_i}{\partial \eta} = \frac{2}{\delta_T}\cdot T_m(\tfrac{1}{2} - \delta) \quad \text{at} \quad \eta = 0,$$

$$T_i = T_m(\tfrac{1}{2} - \delta), \qquad \frac{\partial T_i}{\partial \eta} = -\left.\frac{\mathrm{d}T_m}{\mathrm{d}y}\right|_{y=\frac{1}{2}-\delta} \quad \text{at } \eta = \delta$$

$$T_i = T_m(\tfrac{1}{2} - \delta)\left\{\frac{2}{\zeta}\left(\frac{\eta}{\delta} - 2\frac{\eta^2}{\delta^2} + \frac{\eta^3}{\delta^3}\right) + \left(3\frac{\eta^2}{\delta^2} - 2\frac{\eta^3}{\delta^3}\right)\right\} + \delta\left\{\frac{C_2}{C_1} + \frac{\lambda}{C_1^2}(\tfrac{1}{2} - \delta)\right\} \times \left(\frac{\eta^2}{\delta^2} - \frac{\eta^3}{\delta^3}\right). \quad (81)$$

(b) The temperature distribution in region ii.

Boundary conditions and the distribution of T_{ii} are;

$$T_{ii} = 0, \qquad \frac{\partial T_{ii}}{\partial \xi} = \frac{2}{\delta_T} T_m(y) \quad \text{at} \quad \xi = 0,$$

$$T_{ii} = T_m(y), \qquad \frac{\partial T_{ii}}{\partial \xi} = 0 \quad \text{at} \quad \xi = \delta$$

$$T_{ii} = T_m(y)\left\{\frac{2}{\zeta}\left(\frac{\xi}{\delta} - 2\frac{\xi^2}{\delta^2} + \frac{\xi^3}{\delta^3}\right) + \left(3\frac{\xi^2}{\delta^2} - 2\frac{\xi^3}{\delta^3}\right)\right\}. \quad (82)$$

(c) The temperature distribution in region iii.

Boundary conditions and the distribution of T_{iii} are;

$$T_{iii} = 0, \quad \frac{\partial T_{iii}}{\partial \eta} = \frac{2}{\delta_T} T_m(-\tfrac{1}{2} + \delta) \quad \text{at} \quad \eta = 0,$$

$$T_{iii} = T_m(-\tfrac{1}{2}+\delta), \quad \frac{\partial T_{iii}}{\partial \eta} = \left.\frac{\mathrm{d}T_m}{\mathrm{d}y}\right|_{y=-\frac{1}{2}+\delta} \quad \text{at } \eta = \delta$$

$$T_{iii} = T_m(-\tfrac{1}{2} + \delta)\left\{\frac{2}{\zeta}\left(\frac{\eta}{\delta} - 2\frac{\eta^2}{\delta^2} + \frac{\eta^3}{\delta^3}\right) + \left(3\frac{\eta^2}{\delta^2} - 2\frac{\eta^3}{\delta^3}\right)\right\} - \delta\left\{\frac{C_2}{C_1} - \frac{\lambda}{C_1^2}(\tfrac{1}{2} - \delta)\right\} \times \left(\frac{\eta^2}{\delta^2} - \frac{\eta^3}{\delta^3}\right). \tag{83}$$

2.2.4. *Solution for* C_3 *and* ζ. (1) The case of $\zeta \geqslant 1$. Substituting equations (78)–(80) into equations (76) and (77), and neglecting the higher order terms, we obtain the following equations:

$$C_2\left(C_3 + \frac{\lambda}{8C_1^2}\right) = \frac{8}{3}\frac{1}{\zeta\delta} - \frac{1}{PrRe} \times \left\{2C_3^2 + \frac{1}{3}C_3\frac{\lambda}{C_1^2} + \frac{3}{40}\left(\frac{\lambda}{2C_1^2}\right)^2 + \frac{1}{3}\left(\frac{C_2}{C_1}\right)^2\right\} \tag{84}$$

$$1 = \frac{8}{\zeta\delta}\frac{1}{Pr\,Re}\left(C_3 + \frac{1}{12}\frac{\lambda}{C_1^2}\right). \tag{85}$$

Substituting the values of C_1, C_2, λ and δ, which are given in equations (63)–(66), we obtain the solution for C_3 and ζ.

$$C_3 = 0{\cdot}225\,Re\,K^{-\frac{1}{4}} \tag{86}$$

$$\zeta = 0{\cdot}851\,Pr^{-1} \tag{87}$$

The above results are valid for the range of the Prandtl number smaller than 0·851.

(ii) The case of $\zeta \leqslant 1$.

Substituting equations (81)–(83) into equations (76) and (77), and neglecting the higher order terms, we obtain the following equations:

$$C_2\left(C_3 + \frac{\lambda}{8C_1^2}\right) = \frac{4}{15}\frac{1}{\delta Pr\,Re}\left(\frac{4}{\zeta^2} - \frac{3}{\zeta} + 9\right) \times \left\{2C_3^2 + \frac{1}{3}C_3\frac{\lambda}{C_1^2} + \frac{3}{40}\left(\frac{\lambda}{2C_1^2}\right) + \frac{1}{3}\left(\frac{C_2}{C_1}\right)^2\right\} \tag{88}$$

$$1 = \frac{8}{\zeta\delta}\cdot\frac{1}{Pr\,Re}\left(C_3 + \frac{1}{12}\frac{\lambda}{C_1^2}\right). \tag{89}$$

Substituting equations (63)–(66) into the above equations, we obtain the solutions for C_3 and ζ.

The relation between Pr and $F(Pr)$ is indicated in Table 1.

Table 1. The relation between Pr *and* F(Pr)

Pr	0·851	1	3	10	30	∞
F(Pr)	1	0·739	0·441	0·262	0·253	0·250

$$\zeta = F(Pr) \tag{90}$$

$$C_3 = \frac{(0{\cdot}375\,Pr\,\zeta - 0{\cdot}0937)\,Re}{K^{\frac{1}{4}}} \tag{91}$$

2.2.5. *The Nusselt number.* The Nusselt number is defined by equation (92)

$$Nu = \frac{qd}{k(\boldsymbol{T}_w - \boldsymbol{T}_{mix})} \tag{92}$$

where q is the heat flux at the wall and is written as $q = (\frac{1}{4})k\tau PrRe$. $\boldsymbol{T}_{mix}$ is the mixed mean temperature defined by the following equation:

$$\boldsymbol{T}_{mix} = \frac{1}{d^2\,\overline{U}}\int_{-d/2}^{d/2}\int_{-d/2}^{d/2} \boldsymbol{T}\,U\,\mathrm{d}Y\,\mathrm{d}Z.$$

Substituting the above definitions of q and $\boldsymbol{T}_{mix}$ into equation (92), we can write the Nusselt number as follows:

$$Nu = \frac{Pr\,Re}{4\int_{-\frac{1}{2}}^{\frac{1}{2}}\int_{-\frac{1}{2}}^{\frac{1}{2}} Tu\,\mathrm{d}y\,\mathrm{d}z}. \tag{93}$$

In order to calculate the first approximation of the Nusselt number, the denominator of equation (93) might be written as

$$\int_{-\frac{1}{2}}^{\frac{1}{2}}\int_{-\frac{1}{2}}^{\frac{1}{2}} Tu\,\mathrm{d}y\,\mathrm{d}z \doteqdot \int_{-\frac{1}{2}}^{\frac{1}{2}}\int_{-\frac{1}{2}}^{\frac{1}{2}} T_m(y)\,u_m(y)\,\mathrm{d}y\,\mathrm{d}z.$$

This approximation means that we neglect the existence of the boundary layer. Substituting equations (6) and (75) into the denominator of equation (93), we obtain the following result as the first approximation for the Nusselt number.

$$Nu_1 = \frac{Pr\, K^{\frac{1}{2}}}{4\{0{\cdot}375\, Pr\, \zeta + 0{\cdot}0468\}}. \tag{94}$$

Defining the Nusselt number for a straight square channel under a condition of constant wall temperature gradient by Nu_0 ($Nu_0 = 3{\cdot}63$) and non-dimensionize Nu_1 by Nu_0, we have

$$\frac{Nu_1}{Nu_0} = \frac{0{\cdot}0689\, K^{\frac{1}{2}}}{0{\cdot}375\, \zeta + (0{\cdot}0468/Pr)}. \tag{95}$$

According to the value of the Prandtl number, we must use equation (87) or (90) to calculate the value of ζ in the above equation.

The second approximation for the Nusselt number can be obtained from the consideration of the existence of the boundary layer.

(i) The case of $\zeta \geqslant 1$ ($Pr \leqslant 0{\cdot}851$).

Considering the existence of the boundary layer, we write the denominator of equation (93) as follows:

$$\int_{-\frac{1}{2}}^{\frac{1}{2}}\int_{-\frac{1}{2}}^{\frac{1}{2}} Tu\,\mathrm{d}y\,\mathrm{d}z = 2\int_{0}^{\frac{1}{2}-\zeta\delta}\int_{-\frac{1}{2}+\zeta\delta}^{\frac{1}{2}-\zeta\delta} T_m(y)\,.\,u_m(y)\,\mathrm{d}y\,\mathrm{d}z$$

$$+2\,\Big[\int_{\delta}^{\zeta\delta}\int_{0}^{\frac{1}{2}-\delta} u_m(\eta)\,.\,T_{\mathrm{i}}\,\mathrm{d}\eta\,\mathrm{d}z + \int_{-\frac{1}{2}+\zeta\delta}^{\frac{1}{2}-\zeta\delta}\int_{\delta}^{\zeta\delta} u_m(y)$$

$$\times\; T_{\mathrm{ii}}\,\mathrm{d}y\,\mathrm{d}\xi + \int_{\delta}^{\zeta\delta}\int_{0}^{\frac{1}{2}-\delta} u_m(\eta)\,.\,T_{\mathrm{iii}}\,\mathrm{d}\eta\,\mathrm{d}z$$

$$+\int_{0}^{\delta}\int_{0}^{\frac{1}{2}-\delta} (u_{\mathrm{i}}\,T_{\mathrm{i}} + u_{\mathrm{iii}}\,T_{\mathrm{iii}})\,\mathrm{d}\eta\,\mathrm{d}z$$

$$+\int_{-\frac{1}{2}+\delta}^{\frac{1}{2}-\delta}\int_{0}^{\delta} u_{\mathrm{ii}}\,T_{\mathrm{ii}}\,\mathrm{d}y\,\mathrm{d}\xi\Big].$$

Neglecting the higher order terms which are contained in the boundary layer correction terms, we can calculate the value of the above equation. The distributions of u_{i}, u_{ii}, u_{iii} and T_{i}, T_{ii}, T_{iii} are given by equations (40), (46), (51) and (78)–(80), respectively. The result of the second approximation is given by equation (96)

$$\frac{Nu_2}{Nu_0} = \frac{0{\cdot}0689\, K^{\frac{1}{2}}}{\left\{0{\cdot}375\,\zeta + \dfrac{0{\cdot}0468}{Pr}\right\} - \dfrac{11{\cdot}99}{K^{\frac{1}{2}}}\left\{0{\cdot}375\,\zeta + \dfrac{0{\cdot}187}{Pr}\right\}\left(\dfrac{\zeta}{3} + \dfrac{5\,\zeta - 1}{30\,\zeta^2}\right)} \tag{96}$$

where ζ in the above equation is calculated by equation (87).

(ii) The case of $\zeta \leqslant 1$ ($Pr \geqslant 0{\cdot}851$).

We write the denominator of equation (93) as follows:

$$\int_{-\frac{1}{2}}^{\frac{1}{2}}\int_{-\frac{1}{2}}^{\frac{1}{2}} Tu\,\mathrm{d}y\,\mathrm{d}z = 2\int_{0}^{\frac{1}{2}-\delta}\int_{-\frac{1}{2}+\delta}^{\frac{1}{2}-\delta} T_m(y)\,.\,u_m(y)\,\mathrm{d}y\,\mathrm{d}z$$

$$+\,2\Big[\int_{\frac{1}{2}-\delta}^{\frac{1}{2}}\int_{0}^{\frac{1}{2}-\delta} T_{\mathrm{i}}\,u_{\mathrm{i}}\,\mathrm{d}y\,\mathrm{d}z + \int_{-\frac{1}{2}}^{-\frac{1}{2}+\delta}\int_{0}^{\frac{1}{2}-\delta} T_{\mathrm{iii}}u_{\mathrm{iii}}\,\mathrm{d}y\,\mathrm{d}z$$

$$+\int_{-\frac{1}{2}+\delta}^{\frac{1}{2}-\delta}\int_{\frac{1}{2}-\delta}^{\frac{1}{2}} T_{\mathrm{ii}}\,u_{\mathrm{ii}}\,\mathrm{d}y\,\mathrm{d}z\Big].$$

The distribution of T_{i}, T_{ii} and T_{iii} are given by equations (81)–(83). The result for this case is given as follows:

$$\frac{Nu_2}{Nu_0} = \frac{0{\cdot}0689\, K^{\frac{1}{2}}}{\left\{0{\cdot}375\,\zeta + \dfrac{0{\cdot}0468}{Pr}\right\} - \dfrac{11{\cdot}99}{K^{\frac{1}{2}}}\left\{0{\cdot}375\,\zeta - \dfrac{0{\cdot}187}{Pr}\right\}\left(\dfrac{17}{30} - \dfrac{1}{10\,\zeta}\right)} \tag{97}$$

where we must use equation (9) to calculate the value of ζ.

3. EXPERIMENT

A schematic drawing of the experimental apparatus is shown in Fig. 5. Air flow in a curved square channel, having dimensions of $R = 267$ mm and $d = 20$ mm ($d/R = 0.0714$), is used and the distributions of u and T of the fully developed flow are measured under the condition of a constant wall temperature gradient. The Nusselt number is obtained by use of these distributions.

The upper and the lower walls of the channel (see Fig. 5) are of iron plates with the prescribed dimension, and the inner and the outer walls are of brass plates. These four walls are heated by independent electric heaters so that a constant wall temperature gradient is maintained. The surface temperature of each wall is measured by Cu–Co thermocouples soldered to it. The measured circumferential and flow (axial) directional wall temperature distributions are shown in Fig. 6.

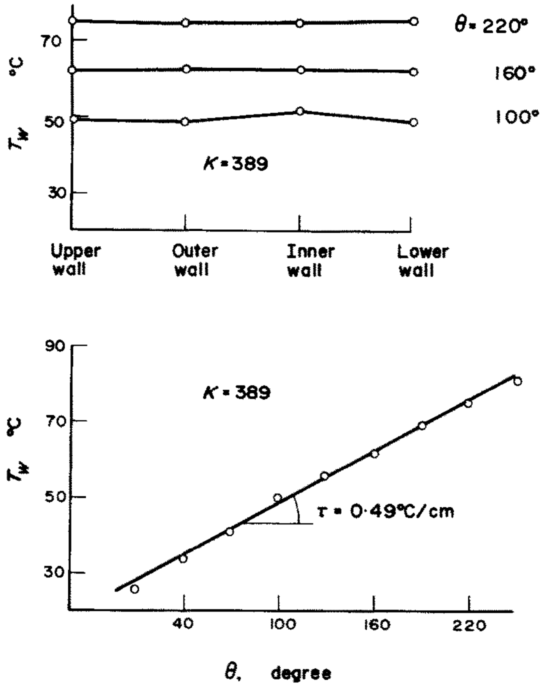

FIG. 6. Wall temperature distribution.

The velocity distribution is measured by a constant current thermistor bead anemometer whose performance between the resistance and the wind velocity is calibrated in advance. Because of the strong temperature dependence of the thermistor resistance, the velocity distribu-

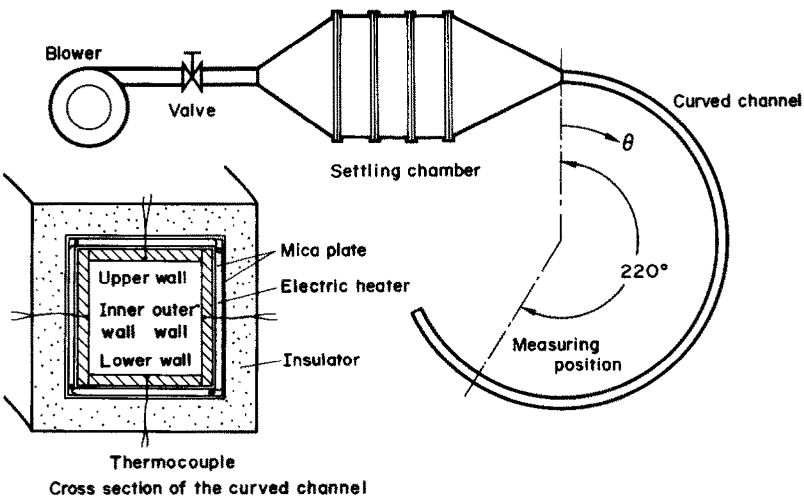

FIG. 5. Experimental apparatus.

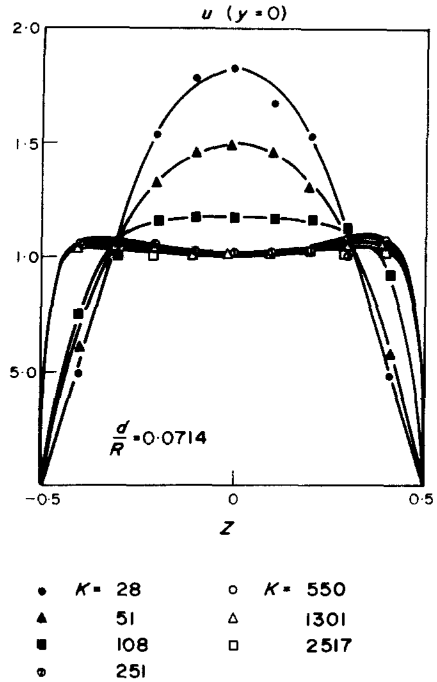

FIG. 7. Distribution of u at $y = 0$.

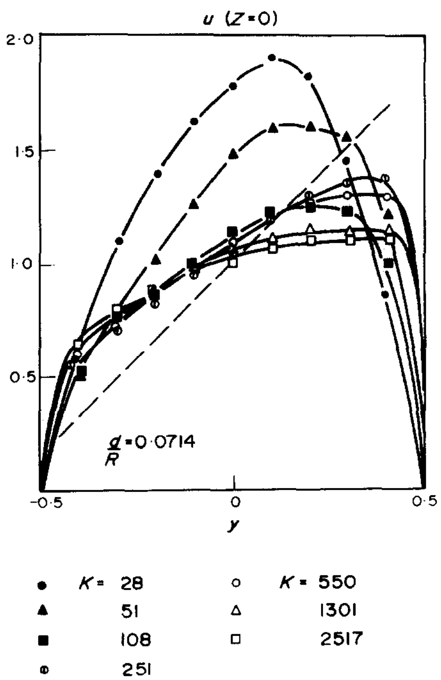

FIG. 8. Distribution of u at $z = 0$.

tion is measured under the condition of zero wall heat flux. The temperature distribution in the channel is measured by a Cu–Co thermocouple of 0·1 mm dia. Lead wires of the thermistor and the thermocouple are in an L-shape support so that the results may not be influenced by a measuring hole.

3.1. *Experimental result*

3.1.1. *The flow field.* The axial velocity distribution, u, is shown in Fig. 7 and 8. The practical flow field is three dimensional due to the secondary flow, and the velocity of $(u^2 + v^2 + w^2)^{\frac{1}{2}}$ is measured by the thermistor anemometer. However, considering $u \gg v, w$, this value may be approximated by u without a serious error.

Figures 7 and 8 respectively indicate the dependency of u at $y = 0$ on z and that at $z = 0$ on y. The maximum value of u is displaced to the centrifugal force direction and the dependency of u on z is weakened with an increase of the Dean number K. For sufficiently large K, these figures show that the gradient of u indicates a rapid change near the wall of the passage. These experimental results mean that we may assume the existence of the velocity boundary layer along the wall in the theoretical analysis. The dotted lines in figures represent the distribution of $u_m(y)$ due to equation (6).

The relation between the resistance coefficient,

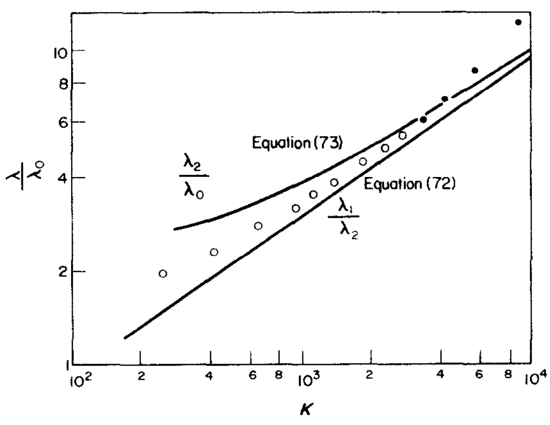

FIG. 9. The resistance coefficient.

λ_1/λ_0 and λ_2/λ_0, and the Dean number K is indicated in Fig. 9. The open circles in the figure are experimental results obtained by H. Ludwieg [4] for a square channel whose R/d equalled 5·67. The figure indicates that analytical and experimental results are in good agreement. The solid circles in the figure indicate experimental results having Reynolds numbers larger than $8{\cdot}0 \times 10^3$ and these are data in a turbulent region. The transition from a laminar to a turbulent flow is measured by a hot-wire. In this experiment, the transition occurs at $K \doteqdot 850$ ($Re \doteqdot 3200$) and the value of the critical Reynolds number is smaller than that measured by H. Ludwieg, i.e. about 8000. The large turbulent intensity at the entrance of the curved channel in our experiment may be responsible for this discrepancy.

The dependency of u on K is weakened after the transition and the velocity distributions hardly deform with an increase in K.

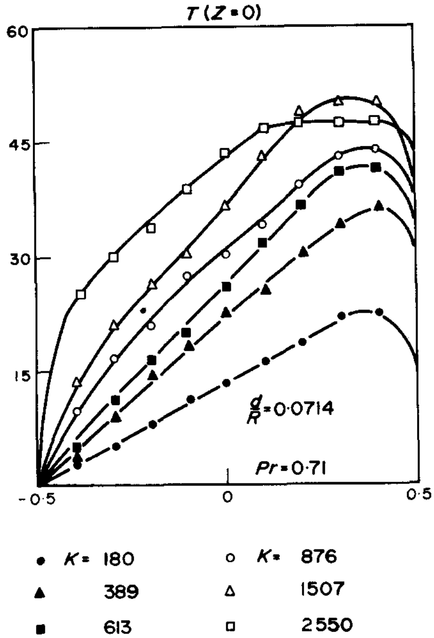

FIG. 11. Distribution of T at $z = 0$.

3.1.2. *The temperature field.* Corresponding with the velocity distribution data, the temperature distributions at $y = 0$ and $z = 0$ are indicated in Figs. 10 and 11, respectively. The same tendency as in the flow field is observed and the validity of the boundary layer approximation is also assured. As mentioned in the preceding section, the distribution of u is hardly deformed with a change of K when K is above 850. Therefore, the distributions of T in the core region are theoretically expected to be similar regardless the value of K. However, the experimental results obtained and shown in Fig. 11 are quite different from the expectation. This disagreement is presumably caused by an actual experimental condition which might be contrary to the condition of the constant circumferential wall temperature at the cross section, adopted in the theory.

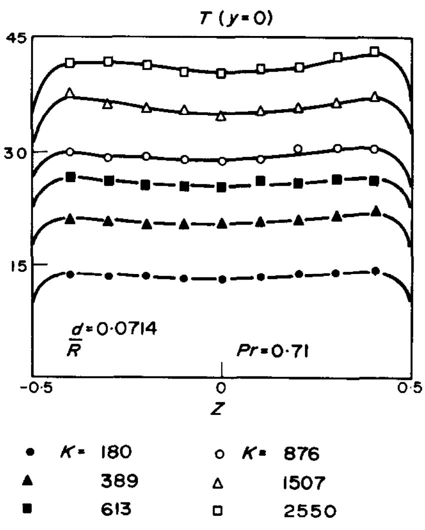

FIG. 10. Distribution of T at $y = 0$.

3.1.3. *The Nusselt number.* The comparison between the analytical and experimental results on the Nusselt number is shown in Fig. 12. The experimental value of the Nusselt number is obtained by use of equation (93). Measured distributions of u and T are substituted into the denominator of equation (93) and this value is calculated by the graphical integration.

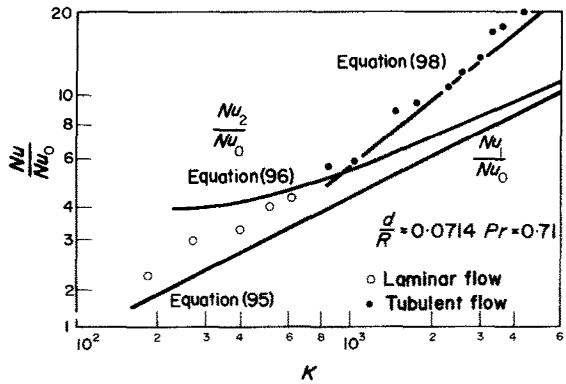

FIG. 12. The Nusselt number.

Open and closed circles in the figure are the experimental results in laminar and turbulent flow regions, respectively. As is shown in the figure, experimental data in a turbulent region can be correlated by equation (98).

$$\frac{Nu}{Nu_0} = 0{\cdot}0208\, K^{\frac{4}{5}}\,.\,(1 + 0{\cdot}287\, K^{-\frac{1}{5}}). \quad (98)$$

Equation (98) is based on the analytical result of a turbulent flow heat transfer in a curved pipe [5], where the hydraulic diameter is used as the reference length instead of the pipe diameter.

4. CONCLUSION

Considering a fully developed laminar flow and temperature fields in a square cross sectional curved channel under the condition of a constant wall temperature gradient, we obtained the following conclusions:

(1) Due to the affect of the centrifugal force, a secondary flow appears in the curved channel. The intensity of the secondary flow increases with the increase of the Dean number $K(K = Re\,.\,\sqrt{d/R})$, and it is possible to consider the existence of the secondary flow boundary layer for the range of the large Dean number when the effect of curvature of the channel cannot be neglected.

(2) We may divide the flow and the temperature fields into two regions, the core and the boundary layer region, and obtain analytical results considering the balance of kinetic energy and entropy production in the boundary layer.

(3) We obtained the resistance coefficient and the Nusselt number for a flow in a square cross sectional curved channel and indicated that these values were seriously increased by the affect of the secondary flow.

(4) Experimental results for the velocity and the temperature distribution were obtained and the Nusselt numbers were calculated using them. Analytical and experimental results were compared with the theoretical prediction and it was found that they were in good agreement.

REFERENCES

1. H. ITO, Theoretical and experimental investigation concerning the flow through curved pipes, *Mem. Inst. High Speed Mech., Tohoku Univ.* **14**, 137–172 (1959).
2. R. A. SEBAN and E. F. MCRAUGHLIN, Heat transfer in tube coils with laminar and turbulent flow, *Int. J. Heat Mass Transfer* **6**, 387–395 (1963).
3. Y. MORI and W. NAKAYAMA, Study on forced convective heat transfer in curved pipes (1st report, laminar region), *Int. J. Heat Mass Transfer* **8**, 67–82 (1965).
4. H. LUDWIGG, Die ausgebildete Kanalströmung in einen rotierenden System, *Ing. Arch.* **19**, 296–305 (1951).
5. Y. MORI and W. NAKAYAMA, Study on forced convective heat transfer in curved pipes (2nd report, turbulent region), *Int. J. Heat Mass Transfer* **10**, 37–59 (1967).

CONVECTION FORCEE THERMIQUE DANS UN CANAL COURBE A SECTION DROITE CARREE

Résumé—On a obtenu sous la condition d'un flux thermique pariétal constant des résultats analytiques et expérimentaux pour un écoulement laminaire entièrement développé dans un canal courbe à section droite carrée. Un écoulement secondaire dû à la force centrifuge apparaît dans le canal et les champs de vitesse et de température sont fortement influencés. Dans le cas d'un écoulement secondaire intense, on a introduit le concept d'une couche limite de l'écoulement secondaire. On a résolu sur la base du bilan d'énergie cinétique et d'entropie les équations du moment et de l'énergie dans la couche limite. On obtient analytiquement et expérimentalement le coefficient de résistance et le nombre de Nusselt et on montre qu'ils sont en bon accord.

ERZWUNGENE KONVEKTIVE WÄRMEÜBERTRAGUNG IN EINEM GEKRÜMMTEN KANAL MIT QUADRATISCHEM QUERSCHNITT.

Zusammenfassung Bei einem gekrümmten Kanal mit quadratischem Querschnitt wurde der Wärmeübergang für den Fall des konstanten Wandwärmestroms für vollausgebildete laminare Strömung analytisch und experimentell untersucht. Verursacht durch die Zentrifugalkraft bildet sich eine Sekundärströmung im Kanal aus, die die Hauptströmung und das Temperaturfeld entscheidend beeinflusst. Im Fall einer intensiven Sekundärströmung wird für die Untersuchung das Grenzschichtmodell für die Sekundärströmung angewandt. Die Bewegungs- und die Energiegleichung für die Grenzschicht werden mit Bilanzen für die kinetische Energie und die Entropieproduktion gelöst. Der Widerstandskoeffizient und die Nusselt-Zahl werden analytisch und experimentell bestimmt und stimmen gut überein.

ВЫНУЖДЕННАЯ КОНВЕКЦИЯ ТЕПЛА В КРИВОЛИНЕЙНОМ КАНАЛЕ КВАДРАТНОГО СЕЧЕНИЯ

Аннотация—Сообщаются результаты аналитического и экспериментального исследований теплообмена при полностью развитом ламинарном течении в криволинейном канале квадратного сечения в условиях постоянного теплового потока на стенке. Благодаря центробежной силе в канале возникает вторичное течение, причем поля скорости и температуры сильно влияют друг на друга. Для интенсивных вторичных течений вводится понятие пограничного слоя вторичного течения. Уравнения двидения и энергии в пограничном слое решаются на основе баланса кинетической энергии и производства энтропии. Аналитическим и экспериментальным путем получены коэффициент гидродинамического сопротивления и число Нуссельта. Констатируется хорошее согласие теории с опытом.